Arab J Sci Eng (2015) 40:2641–2651
DOI 10.1007/s13369-015-1749-z

RESEARCH ARTICLE - ELECTRICAL ENGINEERING

An Efficient ANFIS-Based PI Controller for Maximum Power Point Tracking of PV Systems

M. A. Abido[1] · M. Sheraz Khalid[1] · Muhammed Y. Worku[1]

Received: 19 January 2015 / Accepted: 8 June 2015 / Published online: 25 June 2015

Abstract In this paper, an efficient adaptive neuro-fuzzy inference system (ANFIS)-based PI controller for maximum power point tracking (MPPT) of photovoltaic (PV) systems is proposed. The proposed ANFIS-based MPPT controller has the capacity to track the optimum point under the rapidly changing irradiation conditions with less fluctuations in steady state. The training data of the proposed controller are extracted from a precise PV model developed. The performance of the proposed controller is compared with the conventional incremental conductance method. Finally, the proposed ANFIS-based MPPT controller has been implemented experimentally using real-time digital simulator (RTDS) to simulate a PV system in real time, while the proposed ANFIS-based controller is implemented on dSPACE 1104 controller. Simulation and experimental results show that the proposed ANFIS-based MPPT controller has fast and accurate dynamic response with less fluctuations in steady state. In addition, its performance is superior as compared to the conventional methods.

Keywords Photovoltaic (PV) · Maximum power point tracking (MPPT) · Adaptive network-based fuzzy inference system (ANFIS) · Real-time digital simulator (RTDS) · dSPACE controller

1 Introduction

Among the renewable energy sources, solar energy is the most promising source that can be directly converted to electrical energy using photovoltaic (PV) systems. In 2011, more than 69 GW of PV power is installed worldwide that can generate 85 TWh of electricity per year [1]. The output characteristics of PV array are highly nonlinear and have one peak point called maximum power point (MPP). This optimum point is extremely vulnerable to irradiation and temperature which is always varying with time. Therefore, the MPP tracking (MPPT) controllers are used to trail the optimum point to harvest the maximum possible power from the PV array.

Many MPPT methods have been presented in the literature, and comprehensive comparison of these methods is shown in [2–4]. These techniques have been categorized as online methods and offline methods [3]. Online methods are also called model free methods, as they do not rely on the PV model. This approach includes perturb and observe (P&O) [5], hill climbing (HC) [6] and incremental conductance (InCond) [7,8] techniques. P&O and HC methods are based on the same principle of perturbing the PV system and observing its effect on the PV panel output power. The authors in [9] proved that P&O, HC and InCond methods are actually equivalent, but these techniques suffer from serious drawbacks such as slow tracking of MPP, fluctuation around the MPP in the steady state and failure to track MPP in the rapidly changing atmospheric conditions [10]. All these factors cause considerable amount of power loss. The tracking speed of these techniques can be improved by increasing the perturbation step size, but this in turn causes large fluctuations in the steady state. Trade-off between tracking speed and fluctuations is required that depreciates the performance of these techniques. The problem of tracking in the rapidly changing condition has been resolved by InCond which works on the principle of incrementally comparing the ratio of instantaneous conductance with the derivative of conductance [11]. However, it suffers from the trade-off problem similar to P&O and HC. Many modifications have been car-

✉ Muhammed Y. Worku
muhammedw@kfupm.edu.sa

[1] Department of Electrical Engineering, King Fahd University of Petroleum and Minerals, Dhahran 31261, Saudi Arabia

ried out on these techniques, especially by optimizing the perturbation step size or considering adaptive one [10,12–15]. An adaptive perturbation step size for InCond and P&O has been utilized in [14] and [15], respectively. Theoretical and experimental comparison of P&O and InCond has been investigated in [16] and concluded that both methods have similar performance.

On the other hand, the offline methods comprise of open-circuit voltage (OCV), short-circuit current (SCC) methods [17] and the artificial intelligence (AI)-based methods [18]. OCV and SCC are the most simple and approximate methods. However, these methods are unable to provide the true MPP because of the approximation employed. The AI-based methods are observed to be the most efficient methods since AI has the ability to deal with nonlinear systems [18]. Particle swarm optimization (PSO) as an intelligent technique has been employed to find the MPP and to reduce the fluctuations in the steady state [19]. Fuzzy inference system (FIS) is used to fuzzify the rules of HC method, and artificial neural network (ANN) is employed in [20,21]. Although these techniques show a substantial improvement in tracking the MPP, they are not able to eliminate the fluctuation problem completely.

Adaptive neuro-fuzzy inference system (ANFIS) is proposed to combine the strong features and exhibit the attributes of FIS and ANN [22]. FIS has two major advantages: First, it allows setting the fuzzy rules quite close to the real-world processes, and second, it is interpretable as it can explain the reason of a particular output occurrence. On the other hand, it has some inadequacies such as expert knowledge requirements to define the fuzzy rule base and the computational time to tune the membership function parameters. To build ANFIS-based MPPT controller, the major challenge lies in gathering a large amount of training data. Actual field data for training of ANFIS-based MPPT have been used in [23]. However, several problems are associated with the practical data such as its limited dynamic range. In addition, the collected data are only appropriate for a particular geographical location, and the data collection time should be long enough for better performance of ANFIS.

On the other hand, easy and better way of getting training data is by simulation of PV model as utilized in [24] in which ANFIS-based MPPT is implemented in single-stage topology of power converter (with the inverter only). Open-circuit voltage and short-circuit current as input to the ANFIS MPPT controller are reported in [25], but this technique does not provide the true MPP because of the approximation employed. PV output current and voltage as input to the ANFIS are used in [26–28], whereas irradiation and temperature are used to train the ANFIS MPPT controller in [29,30]. However, the size of the training data used is relatively small that leads to a relatively high training error as reported in [26,27]. In addition, no experimental verification has been reported.

In this paper, a novel MPPT controller is proposed and developed based on ANFIS whose training data are extracted from a precise PV model developed. The proposed controller hybridizes the principles of two efficient intelligent techniques of FIS and ANN. Two-stage topology of power converter is used that provides the flexibility in designing the control architecture. The scheme also offers further advantage by providing the constant DC-link voltage to the inverter, which is beneficial, especially in the case of temperature variations. Results and comparison showed that the proposed ANFIS-based MPPT controller can overcome the shortcomings of the conventional methods and can track the MPP in shorter time with less fluctuations. Competence of the proposed ANFIS-based MPPT controller is verified experimentally where RTDS is used to simulate the PV system in real time and proposed ANFIS-based MPPT controller is developed in dSPACE 1104 controller.

The rest of the paper is organized as follows: Sect. 2 describes the electrical modeling of PV panel and PV array based on the five-parameter model. Proposed ANFIS-based MPPT controller is described in Sect. 3. In Sect. 4, the experimental setup is presented. The Results and discussions are shown in Sect. 5. Finally, Sect. 6 concludes the work.

2 PV Modeling

2.1 PV Panel Modeling

In this study, an efficient five-parameter PV model shown in Fig. 1 is used. The five-parameter model is the most commonly used PV model that produces a close output to that of the practical PV array [31]. This model requires the values of five unknown parameters. These parameters are defined as: -

I_L is the light generated current
I_0 is the reverse saturation current

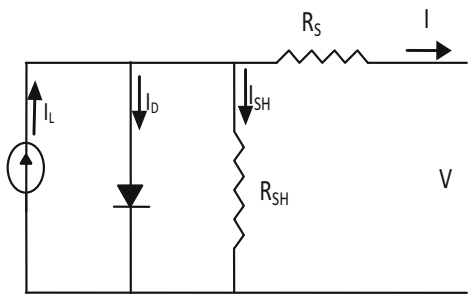

Fig. 1 Equivalent electric circuit of PV device

R_S is the series resistance
R_{SH} is the shunt resistances
"a" is the diode-modified ideality factor

Using simple Kirchhoff's current law, following relationship can be found;

$$I = I_L - I_D - I_{SH} \tag{1}$$

$$I = I_L - I_0 \left\{ \exp\left[\frac{(V + I \times R_S)}{a} \right] - 1 \right\} - \frac{V + I \times R_S}{R_{SH}} \tag{2}$$

where I and V represent the current and voltage generated from the PV panel. I–V characteristics of PV are governed by five parameters (I_L, I_0, R_S, R_{SH} and "a"). If the values of these parameters are known, Eq. (2) can be solved using efficient numerical technique, like Newton–Raphson method. With different atmospheric conditions, these parameters have different values that can be calculated at any ambient condition using the following model translational equations where the series resistance R_s is assumed constant while the shunt resistance R_{SH} varies with irradiation [31].

$$a = a_{ref} \left(\frac{T_c}{T_{c,ref}} \right) \tag{3}$$

$$I_L = \left(\frac{S}{S_{ref}} \right) \left[I_{L,ref} + \mu_{I,sc} \left(T_c - T_{c,ref} \right) \right] \tag{4}$$

$$R_{SH} = R_{SH,ref} \frac{S_{ref}}{S} \tag{5}$$

$$R_S = R_{S,ref} \tag{6}$$

$$\frac{I_0}{I_{0,ref}} = \left(\frac{T_C}{T_{c,ref}} \right)^3 \exp\left(\left(\frac{N_s \times T_{ref}}{a_{ref}} \right) \times \left(\frac{E_{g,ref}}{T_{ref}} - \frac{E_g}{T} \right) \right) \tag{7}$$

$$\frac{E_g}{E_{g,ref}} = 1 - C \left(T - T_{ref} \right) \tag{8}$$

where S and T_c represent the solar radiation and temperature of the PV panel, respectively. $\mu_{I,sc}$ and N_S are the coefficient of short-circuit current and number of cells in the panel, respectively (both of these quantities are provided by the manufacturer). E_g is the band-gap energy of the PV cell material and $C = 0.0003174$ [17]. Quantities with the subscript "*ref*" represent their values at the standard test conditions (STC).

2.2 PV Array Modeling

Large PV power stations are composed of series- and parallel-connected PV panels to increase PV power output. The output current relationship of PV array having N_{SS} series and N_{PP} parallel-connected PV panels can be given by [32];

Table 1 Array parameter value in relation to panel parameters [32]

Panel parameter	Modified array parameters	Model parameter	Modified array parameters
V_{OC}	$V_{OC} \times N_{SS}$	I_L	$I_L \times N_{PP}$
I_{SC}	$I_{SC} \times N_{PP}$	I_0	$I_0 \times N_{PP}$
V_{MP}	$V_{MP} \times N_{SS}$	R_S	$R_S \times (N_{SS}/N_{PP})$
I_{MP}	$I_{MP} \times N_{PP}$	R_{SH}	$R_{SH} \times (N_{SS}/N_{PP})$
n	$n \times N_{SS}$	a	$a \times N_{SS}$

$$I = N_{PP} \times I_L - N_{PP} \times I_0 \left\{ \exp\left[\frac{(V + I R_S \times \mathbb{N})}{N_{SS} \times a} \right] - 1 \right\} - \left(\frac{V + I R_S \times \mathbb{N}}{R_{SH} \times \mathbb{N}} \right) \tag{9}$$

$$\mathbb{N} = \frac{N_{SS}}{N_{PP}} \tag{10}$$

where I_L, I_0, R_S, R_{SH} and "a" are parameters of single PV panel. The relationship of PV array parameters with the PV panel parameters is given in Table 1.

3 Proposed ANFIS-Based MPPT Controller

3.1 ANFIS Structure

ANFIS is based on Takagi–Sugeno-type FIS hypothesis and possesses the learning capabilities of neural network to improve the performance of intelligent system by means of a priori information. ANFIS creates a Fuzzy system and tunes the parameters of the membership function utilizing a certain input–output datasets. Like neural network, ANFIS also has network-type structure and maps the input–output dataset using the parameters of fuzzy membership functions. Figure 2 demonstrates the simple ANFIS architecture based on the two-rule Takagi-Sugeno system with two inputs (x and y) and single output (F). Here A_1, A_2 and B_1, B_2 are fuzzy input memberships for input x and y, respectively.

A two-rule Takagi-Sugeno ANFIS has rules of the form:

$$\text{If } x \text{ is } A_1 \text{ and } y \text{ is } B_1 \quad \text{THEN} \quad f_1 = p_1 x + q_1 y + r_1 \tag{11}$$

$$\text{If } x \text{ is } A_2 \text{ and } y \text{ is } B_2 \quad \text{THEN} \quad f_2 = p_2 x + q_2 y + r_2 \tag{12}$$

where p_i, q_i and r_i are the consequent parameters. Generally, ANFIS architecture has five layers as shown in Fig. 2. Each layer is explained as follows:

Layer 1

In layer 1, every node is adaptive node and their number depends on the number of input membership functions. Their output is given by:

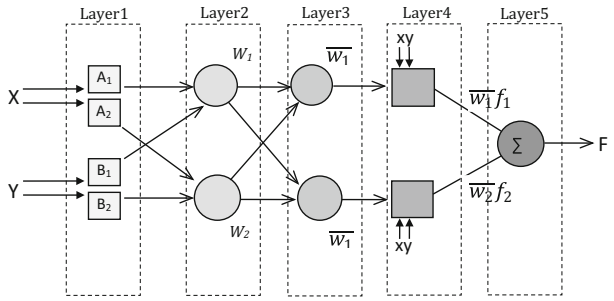

Fig. 2 ANFIS structure

$$O_{1,i} = \mu_{A_i}(x) \quad \text{for} \quad i = 1, 2 \tag{13}$$

$$O_{1,i} = \mu_{B_{i-2}}(y) \quad \text{for} \quad i = 3, 4 \tag{14}$$

where μ is the membership function and $O_{1,i}$ is the membership value for the crisp inputs X and Y. The subscripted 1 and i represent the layer number and node number, respectively.

Membership functions "μ" can be any shaped function like trapezoidal, triangle, and Gaussian. The most commonly used membership function is generalized bell and is given by:

$$\mu_A(x) = \frac{1}{1 + \left|\frac{x - c_i}{a_i}\right|^{2b_i}} \tag{15}$$

where a_i, b_i and c_i are parameters of the membership function (called premise parameter) and need to be optimized in the training process.

Layer 2

Every node in this layer is fixed node and accepts the output (membership values) from layer 1 where t-norm is utilized to "AND" these values, given by;

$$O_{2,i} = w_i = \mu_{A_i}(x)\mu_B(y) \quad i = 1, 2 \tag{16}$$

Output of each node corresponds to the firing strength of a rule.

Layer 3

Every node in this layer is fixed node and used to normalize the firing strength by dividing the rule's firing strength by the sum of all rules' firing strengths, given by;

$$O_{3,i} = \bar{w}_i = \frac{w_i}{w_1 + w_2} \tag{17}$$

Output of each node represents the normalized firing strength of a rule.

Layer 4

Every node in this layer is adaptive node and given by the function;

$$O_{4,i} = \bar{w}_i f_i = \bar{w}_i (p_i x + q_i y + r_i) \tag{18}$$

where p_i, q_i and r_i are the consequent parameters and need to be optimized in the training process.

Layer 5

It has only one fixed node and sums up all the input signals to get the final output and is given by;

$$O_{5,i} = \sum_i \bar{w}_i f_i = \frac{\sum_i w_i f_i}{\sum_i w_i} \tag{19}$$

3.2 ANFIS Learning Process

In the learning algorithm, ANFIS optimizes and adapts its parameters using the training datasets to predict the output data with high accuracy. The Takagi–Sugeno-type model has two types of parameters.

- Nonlinear parameters or membership function parameters (premise parameters).
- Linear parameters or rule parameters (consequent parameters).

The learning method used in this study is based on the hybrid learning algorithm that employs the combination of back-propagation (BP) and least square estimation (LSE) to optimize the premise and consequent parameters [20,33]. In this method, two-pass learning algorithms (forward pass and backward pass) are used:

- In forward pass, consequent (linear) parameters are calculated using a LSE algorithm, while premise (nonlinear) parameters are kept unmodified.
- In backward pass, premise (nonlinear) parameters are calculated using a back-propagation algorithm, while consequent (linear) parameters are kept unmodified.

LSE learning algorithm calculates the square error between training data output and predicted output that is obtained from the Sugeno-type model. This error is utilized to adapt the consequence parameters. The back-propagation gradient descent method uses the error between output training data and predicted output in backward pass to calculate the error in different nodes.

3.3 Application of ANFIS for MPPT

Since the output characteristics of PV system are highly nonlinear, the AI techniques are widely used to improve the efficiency of the MPPT controller. The role of the ANFIS controller proposed in our work is to locate the maximum operating voltage which corresponds to the maximum power of the PV array. It uses the ambient parameters of irradiation and temperature as an input together with the PV array parameters. To design MPPT controller using ANFIS, first task is

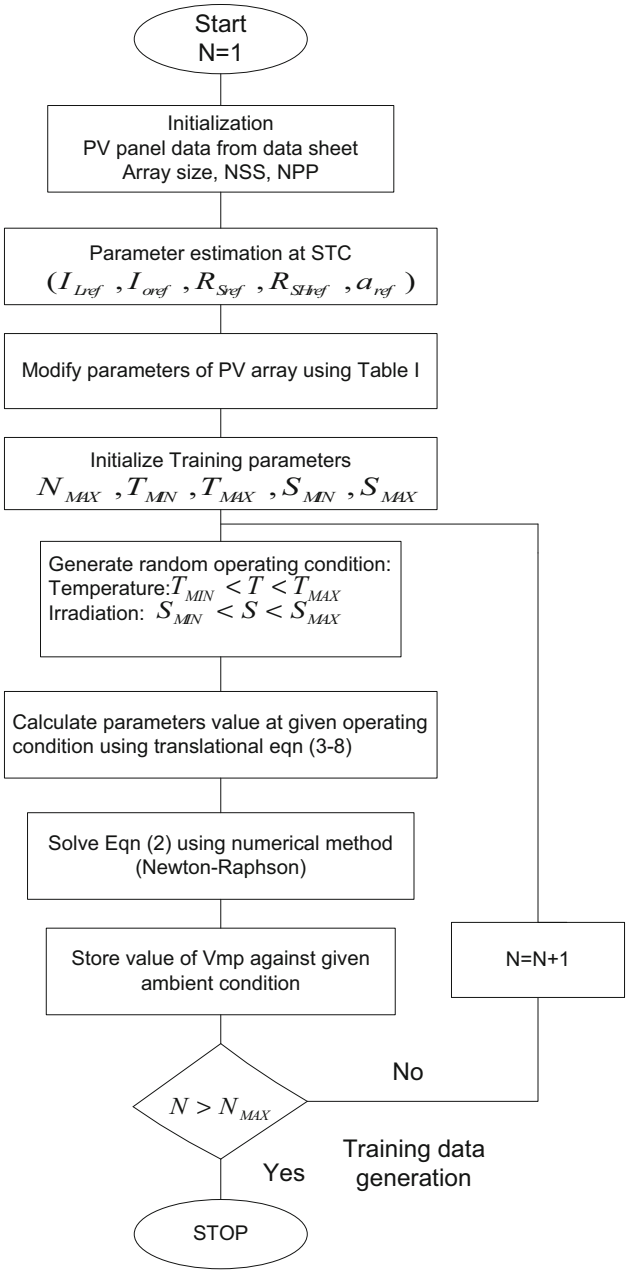

Fig. 3 Proposed method to generate input–output dataset for ANFIS training

to gather the input–output dataset for training purpose. The training data is generated using the efficient PV model developed in [34,35]. A step-by-step process of data generation is illustrated in the flowchart shown in Fig. 3.

As a first step, values of the five unknown parameters for the considered PV panel are estimated and then these values will be transformed for PV array using the parameters given in Table 1. Then, the training parameters are initialized that include;

N_{MAX}: Number of training data points.

T_{MIN}: Minimum temperature
T_{MAX}: Maximum temperature
S_{MIN}: Minimum irradiation
S_{MAX}: Maximum irradiation

where T_{MIN}, T_{MAX} and S_{MIN}, S_{MAX} represent the ranges of temperature and irradiation, respectively. These ranges depend on the geographical location where PV array is installed.

Random operating conditions are generated within the specified ranges and the five parameters at the generated operating conditions are modified using the model translational equations. Then the transcendental nonlinear equation (Eq. 2) is solved using proficient numerical technique of Newton–Raphson method, and the voltage corresponding to the maximum power point is stored against the specified operating condition. This process is executed for N_{MAX} times to generate the training dataset. The ANFIS-based MPPT is designed using the hybrid learning algorithm described above. In the learning algorithm, parameters of the membership functions are adapted such that they track the input–output data accurately.

The arrangement of the developed ANFIS-based MPPT controller is shown in Fig. 4. Once this voltage is located, the PI regulator forces the PV array to work at that voltage by comparing the actual voltage of the PV array and the reference voltage obtained from the ANFIS controller by controlling the duty ratio of the DC–DC converter. The duty cycle of the DC–DC converter is controlled to force the PV array to generate the maximum power. The duty cycle is generated by the PI regulator based on the error between the reference voltage V_{ref} from the ANFIS and the measured PV voltage, V_{PV}.

4 Experimental Setup

Experimentally, the proposed MPPT controller is implemented using dSPACE 1104, which consists of TMS320F240 Digital Signal Processor (DSP) microcontroller. It is based on a 603 PowerPC floating-point processor usually utilized for the designing of digital controllers and real-time simulation purposes [36]. PV system is simulated in real time using real-time digital simulator (RTDS). RTDS is extraordinary computer devised to analyze phenomena of electromagnetic transients in real time.

The process of MPP tracking mainly consists of DC-DC converter switching which is implemented using RTDS. Hardware of the RTDS is based on RISC (reduced instruction set computer) and digital signal processors (DSP) and employs the methods of parallel processing to accomplish the continuous real-time operation [37]. It offers real-time simulation of any number of series and parallel-connected PV

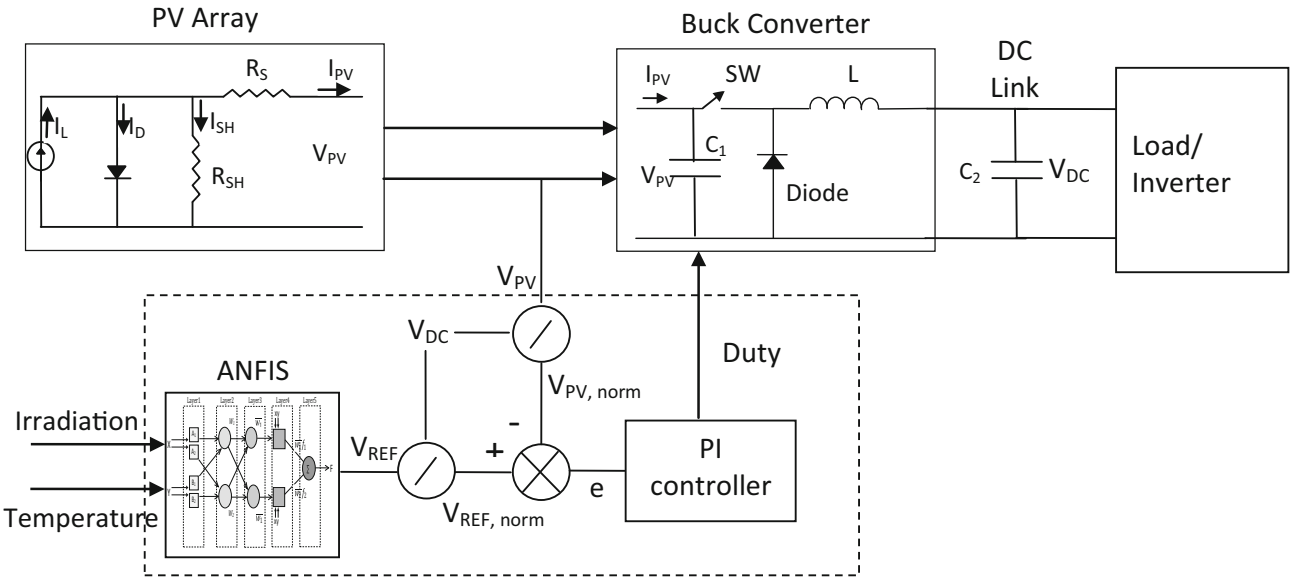

Fig. 4 PV system equipped with the proposed ANFIS-based controller

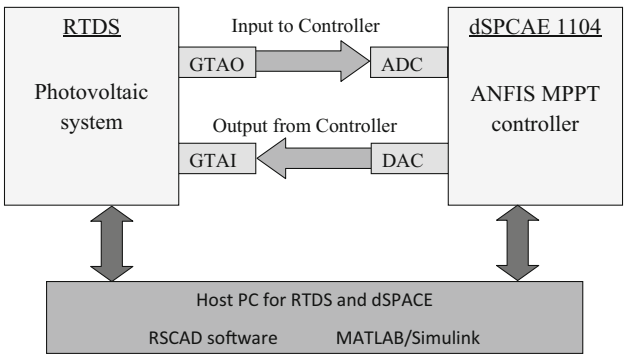

Fig. 5 A schematic diagram of the closed loop control system

panels under different operating conditions. The 16-bit GT Analogue Output (GTAO) and GT Analogue Input (GTAI) cards are installed on the RTDS and used to interface the RTDS with dSPACE 1104. A schematic diagram of the closed loop control system is shown in Fig. 5, and complete experimental setup is shown in Fig. 6.

The proposed ANFIS-based MPPT controller is implemented in dSPACE DS1104, while the PV array and the buck converter are implemented in RTDS. The input irradiation and temperature to the PV array are taken from the RTDS GTAO port and are sent to the dSPACE as input signals. These signals are converted to digital signals using the ADC. The dSPACE controller generates the reference voltage V_{ref} (which is the maximum operating voltage), and the DAC converts this signal to analog signal that is given to the RTDS using the GTAI. The PI regulator implemented in RTDS generates the duty cycle as the input to the buck converter.

5 Results and Discussions

5.1 PV System Specification

Specification of the PV array used is shown in Table 2. An array of 50×20 ($N_{\text{SS}} = 50$ and $N_{\text{PP}} = 20$) panels is used to show the operation of the proposed ANFIS-based MPPT controller with a large PV power station. Buck converter is designed to work in a continuous conduction mode (CCM) and has the following specifications: $C_1 = 100\,\mu\text{F}$, $L = 5\,\text{mH}$, switching frequency 5 kHz and DC-link capacitor $C_2 = 500\,\mu\text{F}$.

5.2 ANFIS Design

Training parameters used to generate the set of input–output data are: $N_{\text{MAX}} = 1000$, $T_{\text{MAX}} = 80\,^{\circ}\text{C}$, $T_{\text{MIN}} = 0\,^{\circ}\text{C}$, $S_{\text{MAX}} = 2000\,\text{W/m}^2$, $S_{\text{MIN}} = 0\,\text{W/m}^2$. These parameters show wide and dynamic range for temperature and irradiation that allows the designed MPPT to work efficiently under uncertain operating conditions.

The ANFIS-based MPPT is developed in MATLAB/Simulink using three generalized bell (g-bell) membership functions. The membership functions are selected by comparing training root-mean-square error for different number of membership function shapes. Hybrid learning algorithm is utilized in this work that uses the LSE to adapt the consequent parameters and back-propagation method to optimize the premise parameters of the membership functions. The root-mean-square error versus epochs during the training process is shown in Fig. 7. It is clear that the proposed approach

Fig. 6 Experimental setup

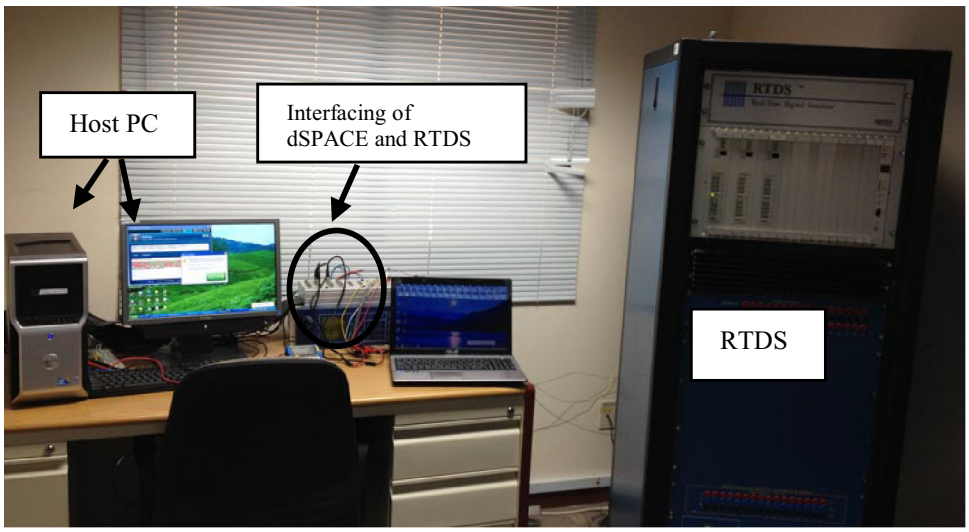

Table 2 Specification of PV array parameter at STC

Parameter	Values
Rated power at MPP (P_{MP})	53.07 kW
Voltage at MPP (V_{MP})	870 V
Current at MPP (I_{MP})	61 A
Open-circuit voltage (V_{OC})	1085 V
Short-circuit current (I_{SC})	67 A
No. of panels connected in series (N_{SS})	50
No. of panels connected in parallel (N_{PP})	20
No. of cells in each panel (N_S)	36

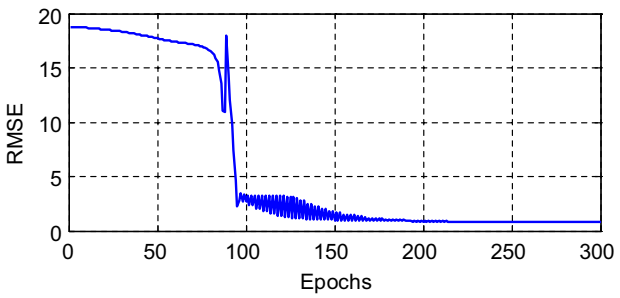

Fig. 7 Training error versus epochs for the ANFIS

for training process is quite efficient as the root-mean-square error is reduced substantially to <4 % within 200 epochs which is by far better than that reported in [27,28,30] that is more than 6 %.

5.3 Validation

To validate the effectiveness of the proposed ANFIS-based MPPT, a comparison with conventional incremental conductance (InCond) method is carried out. Simulation and

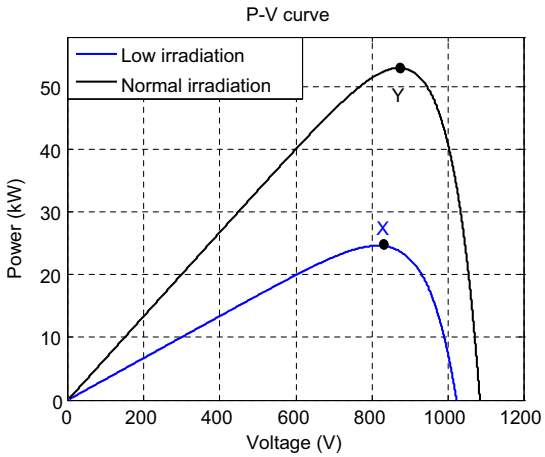

Fig. 8 PV curve under normal and low irradiation conditions

experimental tests are conducted under step-up change in irradiation level. The irradiation is kept constant with a value of 500 W/m^2 up to 0.25 s, and then it increases drastically to 1000 W/m^2. The P-V curves for the selected PV array under low (500 W/m^2 and 25 °C) and normal (1000 W/m^2 and 25 °C) irradiation level are shown in Fig. 8. It can be seen that the maximum power that can be generated by PV array at low irradiation level of 500 W/m^2 is 24.669 kW and labeled as point X on the graph. After a step-up change in irradiation, the operating point shifts to point Y having the maximum possible power, P_{MP}, of 53.07 kW ($V_{MP} \times I_{MP} \times N_{SS} \times N_{PP} =$ 53.07 kW).

5.4 Simulation Results

A nonlinear time domain simulation is carried out with the proposed ANFIS- and InCond-based MPPT controllers. For InCond method, fixed perturbation step size of 0.01 s and an

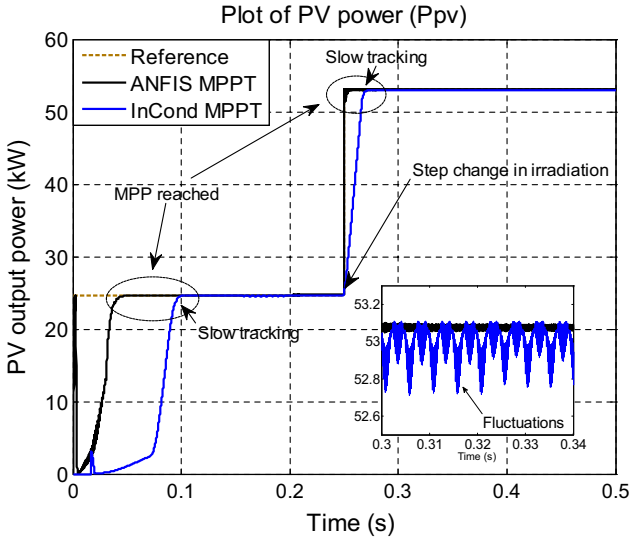

Fig. 9 Characteristics of PV output under step-up irradiation change

update frequency of 20 kHz are chosen based on a trade-off between fluctuations in the steady state and tracking speed. Figure 9 depicts a comparison of PV array power output (P_{PV}) for both controllers. It can be seen that the proposed ANFIS-based MPPT controller is much faster than the conventional InCond at both levels of irradiation. Specifically, the tracking time is 0.04 s with the proposed ANFIS-based MPPT controller, while the InCond controller takes 0.1 s with the first level of irradiation.

To demonstrate the efficiency of a proposed ANFIS-based MPPT controller in steady state, portion of the response from 0.3 to 0.34 s is enlarged with the irradiation level of 1000 W/m^2 as presented in Fig. 9. It is seen from the enlarged portion that the proposed ANFIS-based MPPT has smoother response as compared to InCond, which shows a considerable amount of fluctuations in the steady state. Although, it is possible to diminish these fluctuations by reducing the perturbation step size, but this will result in even more slow tracking response.

The competence of the proposed ANFIS-based MPPT at different operating conditions is illustrated by comparing the maximum power, P_{MP}, extracted by ANFIS-based MPPT with the conventional InCond method. Percentage error is calculated using the reference power from the PV model and is shown in Figs. 10 and 11. Figure 10 presents the percentage error at different irradiation levels with constant temperature of 25 °C, while Fig. 11 shows the error at different temperature with constant irradiation level of 1000 W/m^2. It can be seen that the value of error is negligible for the ANFIS-based MPPT for a wide range of operating conditions. This demonstrates that the proposed controller is able to extract the maximum possible power from the PV array at the considered weather conditions. The simulation results for duty cycle, PV array voltage, V_{PV}, and current, I_{PV}, are shown

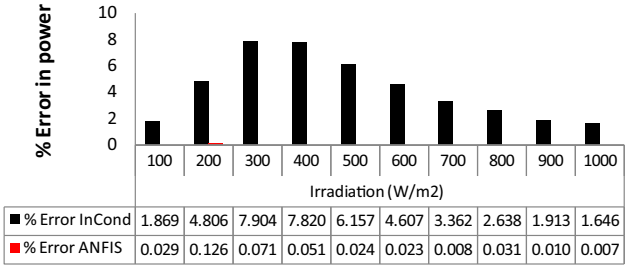

	100	200	300	400	500	600	700	800	900	1000
% Error InCond	1.869	4.806	7.904	7.820	6.157	4.607	3.362	2.638	1.913	1.646
% Error ANFIS	0.029	0.126	0.071	0.051	0.024	0.023	0.008	0.031	0.010	0.007

Fig. 10 Percentage error in P_{MP} at different irradiation level and constant temperature

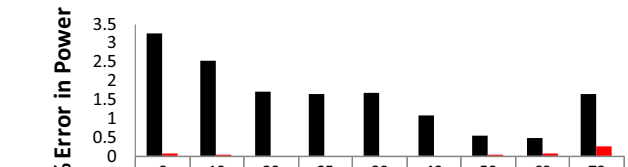

	0	10	20	25	30	40	50	60	70
% Error InCond	3.256	2.516	1.704	1.646	1.683	1.057	0.530	0.472	1.626
% Error ANFIS	0.065	0.036	0.009	0.007	0.007	0.014	0.034	0.068	0.256

Fig. 11 Percentage error in P_{MP} at different temperature and constant irradiation

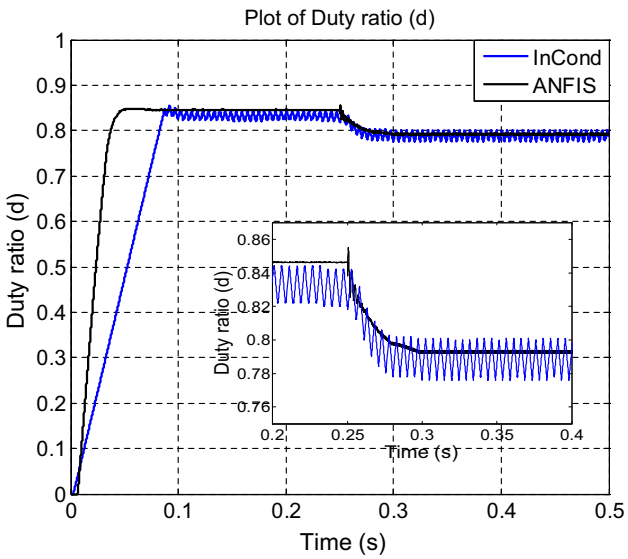

Fig. 12 Duty ratio under step-up irradiation change

in Figs. 12 and 13. The results verify the effectiveness of the proposed ANFIS-based MPPT controller as the fluctuations are almost eliminated compared to InCond controller. From the simulation results discussed, it can be inferred that the response of the proposed ANFIS controller is much faster than that of InCond controller in transitional state and diminishes the oscillations in the steady state.

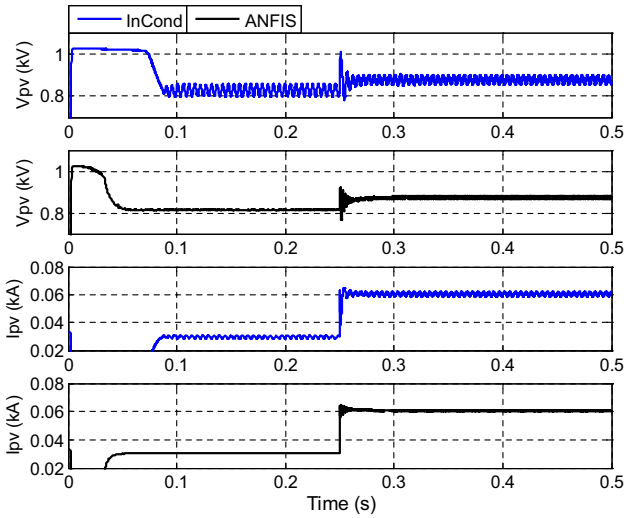

Fig. 13 Characteristics of PV voltage, V_{PV}, and current, I_{PV}

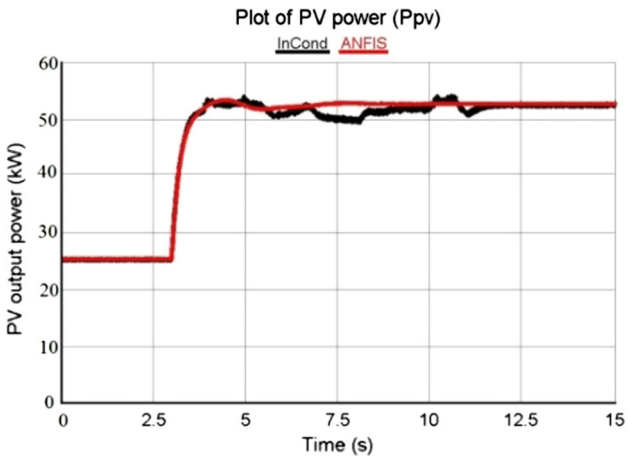

Fig. 14 Experimental waveform for PV power output

5.5 Experimental Results

The experimental setup described in Sect. 4 is utilized to verify the effectiveness of the proposed controller. Step-up change disturbance in irradiation, as used in the simulation, is applied. The responses of P_{PV}, V_{PV}, I_{PV} and duty ratio with the proposed ANFIS controller and InCond controller are shown in Figs. 14 and 15. It can be seen that the proposed controller has better performance with less fluctuations. Also, it can reach the steady state faster than the conventional InCond method. This verifies the competence of the proposed ANFIS-based MPPT over conventional method experimentally.

5.6 Comparison of Simulation and Experimental Results

The results from MATLAB/Simulink simulations are compared with the experimental results to explore the validity of

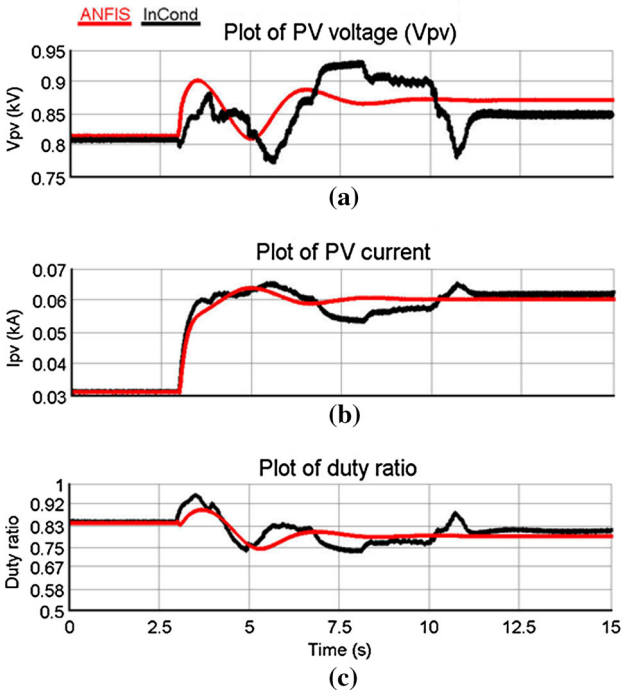

Fig. 15 Experimental waveform for PV voltage, PV current and duty ratio

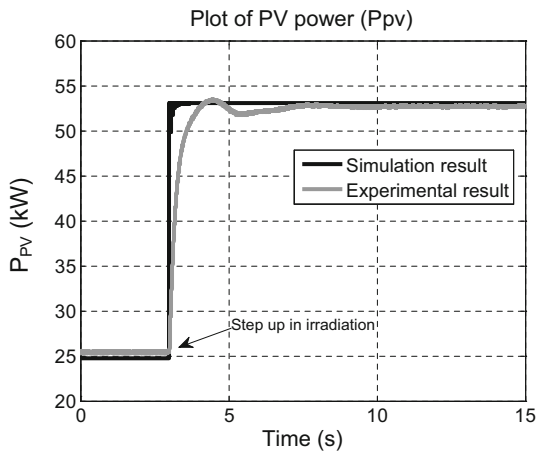

Fig. 16 Comparison of PV power (P_{PV})

the proposed ANFIS-based MPPT controller. A comparison of the system response and performance for the disturbance under discussion is shown in Figs. 16, 17 and 18. Figure 16 depicts the PV power output (P_{PV}) and shows how the proposed controller tracks the MPP in MATLAB/Simulink and experimental simulations under the step-up change in irradiation level. Comparison of V_{PV} and I_{PV} is illustrated in Figs. 17 and 18, respectively. It can be seen that the experimental results are very much close to the simulation results. Both the experimental and MATLAB/Simulink results validate the accuracy of the proposed controller model. However, it is observed that there is some delay in the system response with the experimental results as compared to the simulation

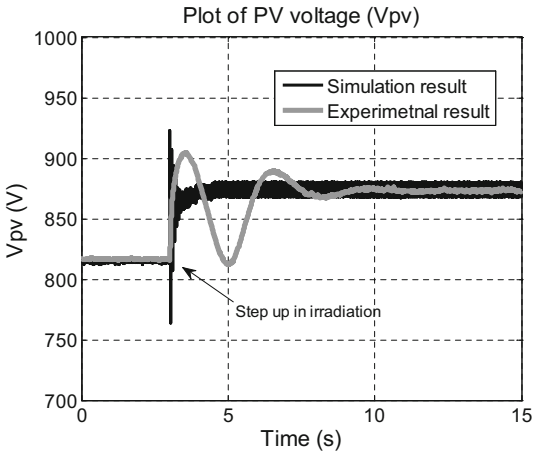

Fig. 17 Comparison of PV voltage (V_{PV})

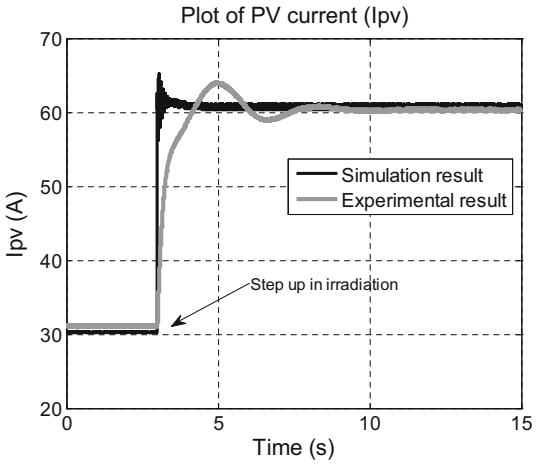

Fig. 18 Comparison of PV current (I_{PV})

results. This can be attributed to the filter implemented in dSPACE to remove the measurement noise and clean the input measurements to the proposed ANFIS controller.

6 Conclusion

In this paper, a proficient ANFIS-based MPPT controller is proposed and developed for PV systems. An efficient and simple approach of training data collection is utilized to improve the tracking efficiency of the proposed MPPT controller. The proposed controller is implemented experimentally and integrated with PV array simulated on RTDS. The simulation results as well as the experimental results show that the proposed ANFIS-based MPPT controller has the fast and accurate response and overcomes the shortcomings of the conventional controllers in terms of the steady-state oscillations. The comparison between simulation and experimental results validates the efficiency of the proposed ANFIS-based MPPT controller.

Acknowledgments The authors acknowledge the support provided by the Deanship of Scientific Research, King Fahd University of Petroleum & Minerals, through Electrical Power and Energy Systems Research Group funded project # RG1207-1&2.

References

1. Global Market Outlook For Photovoltaics Until 2016 *(EPIA)* Industry Association, European Photovoltaic. 2012. [Online]. http://www.epia.org/fileadmin/user_upload/Publications/Global-Market-Outlook-2016.pdf
2. Subudhi, B.; Pradhan, R.: A comparative study on maximum power point tracking techniques for photovoltaic power systems. IEEE Trans. Sustain. Energy **4**(1), 89–98 (2013)
3. Reisi, A. Reza; Moradi, M. Hassan; Jamasb, S.: Classification and comparison of maximum power point tracking techniques for photovoltaic system: a review. Renew. Sustain. Energy Rev. **19**, 433–443 (2013)
4. Esram, T.; Chapman, P.L.: Comparison of photovoltaic array maximum power point tracking techniques. IEEE Trans. Energy Convers. **22**(2), 439–449 (2007)
5. Abdelsalam, A.K.; Massoud, A.M.; Ahmed, S.; Enjeti, P.N.: High-performance adaptive perturb and observe MPPT technique for photovoltaic-based microgrids. IEEE Trans. Power Electron. **26**(4), 1010–1021 (2011)
6. Kjær, S.B.: Evaluation of the 'hill climbing' and the 'incremental conductance' maximum power point trackers for photovoltaic power systems. IEEE Trans. Energy Convers. **27**(4), 922–929 (2012)
7. Safari, A.; Mekhilef, S.: Simulation and hardware implementation of incremental conductance MPPT with direct control method using Cuk converter. IEEE Trans. Ind. Electron. **58**(4), 1154–1161 (2011)
8. Worku, Muhammed. Y.; Abido, M.A.: Real-time implementation of grid-connected PV system with decoupled P-Q controllers. 22nd IEEE Mediterranean Conference of Control and Automation (MED). 841–846 (2014)
9. Sera, D.; Mathe, L.; Kerekes, T.; Spataru, S.V.; Teodorescu, R: On the perturb-and-observe and incremental conductance MPPT methods for PV systems. IEEE J. Photovolt. **3**(3), 1070–1078 (2013)
10. Femia, N.; Petrone, G.; Spagnuolo, G.; Vitelli, M.: Optimization of perturb and observe maximum power point tracking method. IEEE Trans. Power Electron. **20**(4), 963–973 (2005)
11. Elgendy, M.A.; Zahawi, B.; Atkinson, D.J.: Assessment of the incremental conductance maximum power point tracking algorithm. IEEE Trans. Sustain. Energy **4**(1), 108–117 (2013)
12. Sera, D.; Teodorescu, R.; Hantschel, J.; Knoll, M.: Optimized maximum power point tracker for fast-changing environmental conditions. IEEE Trans. Ind. Electron. **55**(7), 2629–2637 (2008)
13. Lee, K.-J.; Kim, R.-Y.: An adaptive maximum power point tracking scheme based on a variable scaling factor for photovoltaic systems. IEEE Trans. Energy Convers. **27**(4), 1002–1008 (2012)
14. Liu, F.; Duan, S.; Liu, F.; Liu, B.; Kang, Y.: A variable step size INC MPPT method for pv systems. IEEE Trans. Ind. Electron. **55**(7), 2622–2628 (2008)
15. Zhang, F.; Thanapalan, K.; Procter, A.; Carr, S.; Maddy, J.: Adaptive hybrid maximum power point tracking method for a photovoltaic system. IEEE Trans. Energy Convers. **28**(2), 353–360 (2013)
16. Sera, D.; Mathe, L.; Kerekes, T.; Spataru, S.V.; Teodorescu, R.: On the perturb-and-observe and incremental conductance MPPT methods for PV systems. IEEE J. Photovolt. **3**(3), 1070–1078 (2013)
17. Masoum, M.A.S.; Dehbonei, H.; Fuchs, E.F.: Theoretical and experimental analyses of photovoltaic systems with voltageand

current-based maximum power-point tracking. IEEE Trans. Energy Convers. **17**(4), 514–522 (2002)
18. Mellit, A.; Kalogirou, S.a.: Artificial intelligence techniques for photovoltaic applications: a review. Prog. Energy Combust. Sci. **34**(5), 574–632 (2008)
19. Ishaque, K.; Salam, Z.; Amjad, M.; Mekhilef, S.: An improved particle swarm optimization (PSO)–based MPPT for PV with reduced steady-state oscillation. IEEE Trans. Power Electron. **27**(8), 3627–3638 (2012)
20. Alajmi, B.N.; Ahmed, K.H.; Finney, S.J.; Williams, B.W.: Fuzzy-logic-control approach of a modified hill-climbing method for maximum power point in microgrid standalone photovoltaic system. IEEE Trans. Power Electron. **26**(4), 1022–1030 (2011)
21. Sheraz, M.; Abido, M.A.: An efficient MPPT controller using differential evolution and neural network. IEEE Int. Conf. Power Energy (PECon). 378–383, (2012)
22. Jang, J.-S.R.: ANFIS: adaptive-network-based fuzzy inference system. IEEE Trans. Syst. Man Cybern. **23**(3), 665–685 (1993)
23. Aldobhani, A.M.S.; John, R.: Maximum power point tracking of PV system using ANFIS prediction and fuzzy logic tracking. Int. MultiConference Eng. Comput. Sci. (IMECS). **2**, 19–21.(2008)
24. Abu-Rub, H.; Iqbal, A.; Moin Ahmed, S.; Peng, F.Z.; Li, Y.; Baoming, G.: Quasi-Z-source inverter-based photovoltaic generation system with maximum power tracking control using ANFIS. IEEE Trans. Sustain. Energy **4**(1), 11–20 (2013)
25. Afghoul, H.; Krim, F.; Chikouche, D.: Increase the photovoltaic conversion efficiency using neuro-fuzzy control applied to MPPT. Renew. Sustain. Energy Conf. (IRSEC). 348–353 (2013)
26. Khaehintung, N.; Sirisuk P.; Kurutach, W.: A novel ANFIS controller for maximum power point tracking in photovoltaic systems. The Fifth International Conference on Power Electronics and Drive Systems, PEDS. 833–836 (2003)
27. Mayssa, F.; Sbita, L.: Advanced ANFIS-MPPT control algorithm for sunshine photovoltaic pumping systems. First International Conference Renewable Energies and Vehicular Technology (REVET). 167–172 (2012)
28. Tarek, B.; Said, D.; Benbouzid, M.E.H.: Maximum power point tracking control for photovoltaic system using adaptive neuro-fuzzy "ANFIS". 8th International Conference and Exhibition on Ecological Vehicles and Renewable Energies (EVER). 1–7 (2013)
29. Iqbal, A.; Abu-Rub, H.; Ahmed, S.M.: Adaptive neuro-fuzzy inference system based maximum power point tracking of a solar PV module. IEEE International Energy Conference and Exhibition (EnergyCon). 51–56 (2010)
30. Kharb, Ravinder Kumar; Shimi, S.L.; Chatterji, S.; Ansari, Md. Fahim: Modeling of solar PV module and maximum power point tracking using ANFIS. Renew. Sustain. Energy Rev. **33**, 602–612 (2014)
31. De Soto, W.; Klein, S.a.; Beckman, W.a.: Improvement and validation of a model for photovoltaic array performance. Sol. Energy **80**(1), 78–88 (2006)
32. Chatterjee, A.; Keyhani, A.; Kapoor, D.: Identification of photovoltaic source models. IEEE Trans. Energy Convers. **26**(3), 883–889 (2011)
33. Jang, J.-S.R.: Neuro-fuzzy modeling and control. Proc. IEEE **83**(3), 378–406 (1995)
34. Siddiqui, M.U.; Abido, M.A.: Parameter estimation for five- and seven-parameter photovoltaic electrical models using evolutionary algorithms. Appl. Soft Comput. **13**(12), 4608–4621 (2013)
35. Khalid, M. Sheraz; Abido, M.A.: A novel and accurate photovoltaic simulator based on seven-parameter model. Electric Power Syst. Res. **116**, 243–251 (2014)
36. User's Manual; DSpace DS1104. www.dspace.com/en/pub/home/products/hw/singbord/ds1104.cfm
37. User's Manual; Real Time Digital Simulator (RTDS). http://www.rtds.com/index/index.html